


# MMP-9 metalloproteinase and its regulator are not associated with mid-term CT residual abnormalities in patients with COVID-19 pneumonia

Acta Radiologica Open  
14(4) 1–8  
© The Author(s) 2025  
Article reuse guidelines:  
[sagepub.com/journals-permissions](https://sagepub.com/journals-permissions)  
DOI: 10.1177/20584601251330563  
[journals.sagepub.com/home/arr](https://journals.sagepub.com/home/arr)  


Monica Mattone<sup>1</sup>, Giorgio Maria Masci<sup>1</sup>, Nicholas Landini<sup>1</sup> ,  
Maria Antonella Zingaropoli<sup>2</sup>, Carlo Catalano<sup>1</sup>, Maria Rosa Ciardi<sup>2</sup> and  
Valeria Panebianco<sup>1</sup>

## Abstract

**Background:** COVID-19 patients may have residual pulmonary alterations after the acute disease, with fibrotic-like alterations. Since metalloproteinases (MMP) and their regulators may be involved in inflammation and abnormal repair processing, we aimed to investigate the correlations between MMP-9, a tissue inhibitor of metalloproteinases (TIMP-1) and chest CT abnormalities in acute phase and mid-term follow-up.

**Methods:** COVID-19 patients with plasma analyses and CT scans performed at acute onset and 3 months after discharge (T post) were evaluated. MMP-9, TIMP-1, and MMP-9/TIMP-1 ratio were analyzed. CT extents of COVID-19 pneumonia and fibrotic-like alterations were visually scored (score range 0–25). Spearman rank correlation analysis ( $p$ -value  $< .05$ ) was computed between acute and mid-term plasma analyses and CT scores.

**Results:** 39 patients were enrolled. At hospital admission, MMP-9, TIMP-1, and MMP-9/TIMP-1 had a median of 240.5 ng/mL, 258.8 ng/mL, and 0.9. The median CT global and fibrotic-like scores were 9 and 6. At T post, MMP-9 and TIMP-1 were not statistically different ( $p$ -value  $< .05$ ). There was a reduction of CT global score ( $p$ -value = .00007). A significant correlation was found between MMP-9 and CT global score at hospital admission ( $\rho = 0.456$ ,  $p$ -value = .003) and between MMP-9/TIMP-1 ratio and CT global score at hospital admission ( $\rho = 0.406$ ,  $p$ -value = .009). No other significant correlations were found between plasma enzymes and CT alterations, both in acute and mid-term follow-up.

**Conclusion:** MMP-9 plasma levels and MMP-9/TIMP-1 ratio correlate with lung involvement during the acute phase. None of the levels of MMP-9, TIMP-1, and MMP-9/TIMP-1 ratio may be adopted as predictors of residual pulmonary alterations in mid-term follow-up.

## Keywords

COVID-19, matrix metalloproteinases, computed tomography, ELISA, MMP-9, TIMP-1

Received 9 January 2025; accepted 12 March 2025

<sup>1</sup>Department of Radiological Sciences, Oncology and Pathology, Policlinico Umberto I, “Sapienza” University, Rome, Italy

<sup>2</sup>Department of Public Health and Infectious Diseases, Policlinico Umberto I, “Sapienza” University, Rome, Italy

## Corresponding author:

Nicholas Landini, Department of Radiological Sciences, Oncology and Pathology, Policlinico Umberto I, “Sapienza” University, Via del Policlinico 161, Rome 00161, Italy.

Email: [nicholas.landini@uniroma1.it](mailto:nicholas.landini@uniroma1.it)



Creative Commons Non Commercial CC BY-NC: This article is distributed under the terms of the Creative Commons Attribution-NonCommercial 4.0 License (<https://creativecommons.org/licenses/by-nc/4.0/>) which permits non-commercial use, reproduction and distribution of the work without further permission provided the original work is attributed as specified on the SAGE and Open Access pages (<https://us.sagepub.com/en-us/nam/open-access-at-sage>).

## Introduction

A common manifestation of COVID-19 is lung involvement, often in the form of pneumonia. Of all patients with COVID-19 infection, approximately 15% may develop a severe illness, requiring hospitalization and oxygen therapy,<sup>1</sup> while 5% may progress to a critical condition, developing multiorgan failure, acute lung injury, or acute respiratory distress syndrome, necessitating admission to the intensive care unit.<sup>2</sup> There is evidence supporting vascular damage and immunothrombosis as key factors involved in the pathogenetic mechanisms of severe forms of COVID-19. Postmortem histopathological examinations have revealed diffuse alveolar damage with perivascular infiltration of inflammatory cells, extensive damage to the lining of blood vessels, severe endothelial injury, and thrombosis.<sup>3–5</sup> A key factor in these mechanisms is the dysregulation of neutrophil extracellular trap (NET). In fact, there is a robust correlation between neutrophil extracellular trap (NET) and severity of respiratory illness.<sup>6</sup> Activated neutrophils release metalloproteinases (MMPs), a large family of zinc-dependent endopeptidases involved in extracellular matrix (ECM) degradation. These enzymes are inhibited by binding or interactions with tissue inhibitors of metalloproteinases (TIMPs). MMPs, whose expression and activation are increased by cytokines such as IL-1 and TNF- $\alpha$ , contribute to the “cytokine storm,” supporting the migration of immune cells to infection sites and promoting platelet and neutrophil activation.<sup>7–11</sup> There are 25 members of this family, involved in different neutrophil extracellular trap (NET) changes. For instance, MMP-3 and MMP-9 can promote abnormal repairing process, MMP-7 and MMP-8 may influence the pulmonary levels of profibrotic/antifibrotic mediators, and MMP-8 and MMP-10 are involved in the pulmonary macrophage regulation.<sup>12</sup> Thus, the NET state depends, at least partially, from the different expression of MMPs and TIMPs.

Considering the severe form of COVID-19 as a septic state, MMP-2 and MMP-9 have been proposed as potential biomarkers of disease severity, including for their possible role as therapeutic targets.<sup>13–15</sup> In fact, several studies have shown increased MMP-9 levels in critical patients, with higher levels of MMP-9 observed in patients with acute respiratory distress syndrome compared to those with non-severe COVID-19.<sup>16,17</sup> Conversely, MMP-2 levels were found to be lower.<sup>18</sup>

On the other hand, although chest computed tomography (CT) is considered non-specific for evaluating COVID-19-related pneumonia, it has shown high sensitivity for detecting parenchymal alterations and, therefore, represents the best imaging tool for assessing the degree of lung involvement.<sup>19</sup> Moreover, several CT scoring systems have been proposed to quantify the extent of pneumonia, both using semi-quantitative methods and automated tools.<sup>20–22</sup>

Furthermore, CT has proven useful in the follow-up of COVID-19-related alterations. For instance, CT abnormalities may resolve after the acute phase or may progress to so-called fibrotic-like alterations, which are parenchymal abnormalities with signs that may be related to fibrosis but can improve over time.<sup>23</sup> However, the underlying factors that may lead to these different outcomes remain unclear. Since MMP activity may be involved in tissue repair and fibrotic processes, we hypothesized that their levels might be related to the different evolution of COVID-19 pneumonia, though few data are available in the literature.<sup>24</sup>

Thus, the aim of this study was to investigate whether MMP and TIMP levels could serve as potential biomarkers of fibrotic-like alterations in COVID-19 patients during mid-term follow-up.

## Materials and methods

### Study design

This single-center retrospective study was conducted at the Department of Radiological Sciences, Oncology and Pathology, Policlinico Umberto I Hospital, “Sapienza” University of Rome. Patients with a confirmed diagnosis of COVID-19 pneumonia, admitted to the hospital between March and June 2020, were considered for enrollment. Inclusion criteria included CT and plasma tests performed at hospital admission and the same examinations repeated 90 days later.

The diagnosis of COVID-19 infection was confirmed using a nasopharyngeal swab and a commercial reverse transcription-polymerase chain reaction (RT-PCR) kit, following the manufacturer’s instructions (RealStar® SARS-CoV-2 Altona Diagnostics, Hamburg, Germany).

The following clinical and laboratory data were collected: age, sex, comorbidities, symptoms and acute respiratory distress syndrome development, and COVID-19 treatment.

This study received approval from the local ethics committee (Lazio, Area 1, Rif. 7226, Prot. 0473/2024). The need for informed consent was waived due to the retrospective nature of the study.

During the acquisition and processing of data, national and international regulations were adhered to.

### Blood test for plasma enzymes

Peripheral whole blood samples were evaluated using a Microfluidic Next Generation Enzyme-Linked Immunosorbent Assay (ELISA) to separately determine the levels of MMP-9 and TIMP-1, using the Simple Plex™ Ella Assay (ProteinSimple, San Jose, CA, USA) on the Ella™ Microfluidic System (Bio-Techne, Minneapolis, MN, USA), according to the

manufacturer's instructions and as previously described.<sup>25–27</sup> Then, the MM-9/TIMP-1 ratio was computed.

### Chest CT analysis

Pulmonary involvement was evaluated by a chest radiologist on axial CT images reconstructed with a sharp kernel and standard lung window, using a semi-quantitative score, as proposed in previous studies.<sup>28,29</sup> The score was visually calculated for each of the five lobes, considering the extent of anatomical involvement, as follows: 0, no involvement; 1, <5% involvement; 2, 5–25% involvement; 3, 26–50% involvement; 4, 51–75% involvement; and 5, >75% involvement. The resulting global CT score was the sum of each individual lobar score and ranged from 0 (no involvement) to 25 (maximum involvement).<sup>30,31</sup> The prevalent parenchymal alterations were also evaluated, including ground-glass opacity, consolidation, crazy paving, and reticulation. The score was also used to assess fibrotic-like alterations, defined by the association of pulmonary abnormalities with architectural distortions, bronchial dilation, volume loss, or honeycombing,<sup>32–35</sup> independently computed.

### Statistical analysis

Data were analyzed using statistical software (Prism version 9, GraphPad Software). Continuous variables were expressed as the median and interquartile range (IQR), while categorical variables were expressed as counts and percentages. Patient characteristics were compared using Student's *t* test or 2-tailed  $\chi^2$  test for continuous and categorical variables, respectively. The 2-tailed  $\chi^2$  test or Fisher's exact test and the nonparametric Mann–Whitney test were used for comparing proportions and medians. Longitudinal evaluation was performed using the nonparametric Wilcoxon test. The relationship between clinical metalloproteinase plasma levels was assessed using Spearman rank correlation analysis. A *p*-value <.05 was considered statistically significant.

## Results

### Patients' characteristics

Thirty-nine out of 52 selected patients met the inclusion criteria and were enrolled. 25 patients were male (64%), and the median age of patients was 64 years, with an interquartile range (IQR) of 55–77. The median follow-up duration was 97 days (IQR: 82–106). Hypertension was the most common comorbidity (41.0%), followed by other cardiovascular diseases (20.6%), diabetes (17.9%), and pulmonary disease, such as COPD and asthma (17.9%). The most used treatment was hydroxychloroquine (69.2%). At

hospital admission, 46.5% of COVID-19 patients developed ARDS. At hospital admission, the most common symptoms were fever (79.5%), cough (41.0%), and shortness of breath (33.3%). All patients' characteristics are shown in Table 1.

### Plasma levels of MMP-9 and TIMP-1

At hospital admission, the ELISA test revealed a median value for MMP-9 of 240.5 ng/mL (IQR: 694.5) and for TIMP-1 of 258 ng/mL (IQR: 314.5), respectively. The median MMP-9/TIMP-1 ratio was 0.9 (IQR: 4). At time post-admission (T post), the plasmatic level of MMP-9 had a median value of 508.3 ng/mL (IQR: 852.25; *p*-value = .95). The plasmatic levels of TIMP-1 were 202.4 ng/mL (IQR: 205.75; *p*-value = .26), and the MMP-9/TIMP-1 ratio had a median value of 2.5 (IQR: 2; *p*-value = .17). Plasma analyses are shown in Table 2.

### CT analysis and correlations with plasma enzymes

In the acute phase of the infection, the median CT global score was 9 (IQR: 5.5), and the most prevalent parenchymal alteration was ground-glass appearance (46.2%), followed by consolidation (33.3%), crazy paving (17.9%), and reticulation (2.6%) (Figure 1). At hospital admission, the median fibrotic-like CT score was 6 (IQR: 4.5). The most common pattern associated with fibrotic-like alterations was consolidation (28.2%), followed by ground-glass appearance (25.6%), crazy paving (17.9%), and reticulation (5.1%).

After 3 months, a significant reduction in the chest CT global score was observed compared to baseline (*p*-value = .00007), with a median score of 5.2 (IQR: 8.5). The most common parenchymal alteration was ground-glass appearance (84.7%), followed by crazy paving (5.1%) and reticulation (5.1%). At T post, the median fibrotic-like score was 3 (IQR: 5.5; *p*-value = .11), and the most common prevalent pattern was ground-glass appearance (48.7%), followed by consolidation (10.3%) and reticulation (5.1%). The most common parenchymal fibrotic alteration at T post was distortion (56.4%) (Figure 1). CT scores are shown in Table 3.

At hospital admission, a positive correlation was found between plasma levels of MMP-9 and the global chest CT score ( $\rho = 0.456$ , *p*-value = .003), and between the MMP-9/TIMP-1 ratio and the CT global score ( $\rho = 0.406$ , *p*-value = .009). Scatter plots are reported in Figure 2. No other significant correlations were found, especially between plasma levels of MMP-9 and MMP-9/TIMP-1 at baseline and chest CT scores at T post (Tables 4 and 5). Regarding the differences between baseline and T post, the only significant difference was found for the  $\Delta$ CT global score, but there were no significant correlations with MMP-9, TIMP-1, and MMP-9/TIMP-1 in the acute phase ( $\rho = -0.135$ , *p*-value = .407 for MMP-9;  $\rho = 0.207$ ,

**Table 1.** Demographic and clinical characteristics of patients.

Number of patients	39
Male/female	25/39 (64%)
Age, median (IQR)	64 (55–77)
Comorbidities	26 (66.7%)
• Hypertension	• 16 (41.0%)
• Other cardiovascular	• 8 (20.6%)
• Diabetes	• 7 (17.9%)
• Pulmonary	• 7 (17.9%)
• Cancer	• 4 (10.3%)
• Other	• 2 (5.2%)
Symptoms	39/39 (100%)
• ARDS	• 18 (46.5%)
• Fever	• 31 (79.5%)
• Cough	• 16 (41.0%)
• Shortness of breath	• 13 (33.3%)
• Myalgia/arthralgia	• 9 (23.0%)
• Diarrhea	• 5 (12.8%)
• Anosmia/ageusia	• 2 (5.12%)
• Sputum production	• 1 (2.5%)
COVID-19 treatment	37/39 (94.8%)
• Lopinavir/ritonavir	• 10 (25.6%)
• Hydroxychloroquine	• 27 (69.2%)
• Azithromycin	• 21 (53.9%)
• Enoxaparin	• 16 (41.0%)
• Corticosteroids	• 12 (30.7%)
• Tocilizumab	• 16 (41.0%)

ARDS: acute respiratory distress syndrome; CT: computed tomography; IQR: interquartile range.

**Table 2.** Next generation ELISA, zymography data, and differences between hospital admission and after discharge. Data are shown as the median and interquartile range (IQR).

Plasma analysis	Baseline	3 months	p-value
ELISA			
MMP-9 (ng/mL)	240.5 (694.5)	508.3 (852.25)	.95
TIMP-1 (ng/mL)	258 (314.5)	202.4 (205.75)	.26
MMP-9/TIMP-1	0.9 (4)	2.5 (3)	.17

ELISA: enzyme-linked immunosorbent assay; MMP-2: matrix metalloproteinase-2; MMP-9: matrix metalloproteinase-9; TIMP-1: tissue inhibitor of metalloproteinase-1.

$p$ -value = .199 for TIMP-1; and  $p$  = 0.078,  $p$ -value = .634) or at T post ( $p$  = −0.019,  $p$ -value = .911 for MMP-9;  $p$  = −0.031,  $p$ -value = .854 for TIMP-1; and  $p$  = 0.083,  $p$ -value = .620).

## Discussion

In our study, MMP-9 and MMP-9/TIMP-1 were elevated among COVID-19 patients and associated with COVID-19 severity, in line with previously observed MMPs.<sup>36,37</sup>

The role of chest CT as a primary imaging tool in the diagnosis and management of COVID-19 has been widely discussed, including the need for standardized radiological reports using various visual scores.<sup>38–40</sup> As described, SARS-CoV-2 stimulates the immune system, leading to a cytokine storm,<sup>41</sup> and COVID-19 pneumonia may be associated with massive alveolar damage and loss of lung architecture. This occurs through an alteration of the NET balance influenced by the different expressions and plasma activities of MMPs and TIMPs. More specifically, MMP-9 induces inflammation and degradation of the alveolar-capillary barrier, stimulating the migration of inflammatory cells and destruction of lung tissue,<sup>42</sup> while TIMP-1 is a specific inhibitor of NET degradation enzymes, promoting fibroblast proliferation and exhibiting antiapoptotic and proinflammatory effects.<sup>42,43</sup> Thus, the MMP-9/TIMP-1 ratio also plays a crucial role, considering the need for balance in lung tissue damage and repair. Various studies have demonstrated the role of MMP-9 levels and the MMP-9/TIMP-1 ratio in the development of community-acquired pneumonia compared to healthy patients, also showing their relationship to the severity of community-acquired pneumonia.<sup>43</sup> Moreover, Demir et al. revealed higher levels of MMP-9 and TIMP-1 in patients with lung involvement on chest CT scans than in those with no lung involvement, without significant differences related to the extent and severity of lung involvement.<sup>42</sup>

However, in our study, plasma levels of MMP-9, TIMP-1, and the MMP-9/TIMP-1 ratio did not correlate with mid-term follow-up CT alterations.

Hence, these results suggest that the plasma enzymes we investigated cannot be adopted as predictors or biomarkers of residual mid-term CT alterations. Since metalloproteinases may be involved in abnormal repair processes,<sup>12</sup> the process underlying the absence of complete restitutio ad integrum after the acute onset seems unrelated to these enzymes. COVID-19 pneumonia typically has a natural course of about 2 to 3 weeks, with described CT alterations such as ground-glass opacities, consolidations, reticulations, and crazy paving.<sup>44</sup> After the acute onset, either complete restitution or residual abnormalities on CT have been observed in survivors. These residual abnormalities may be associated with signs commonly related to fibrosis, such as architectural distortions or bronchiectasis, leading radiologists to describe them as scars or residual fibrotic interstitial lung disease. However, although these alterations were observed several months to even years after the acute onset, they can reduce over time, as observed in previous SARS-MERS infections. For this reason, the term “fibrotic-like changes” was coined for residual parenchymal abnormalities in COVID-19 pneumonia with apparent signs of fibrosis, such as bronchial dilation instead of apparent traction bronchiectasis.<sup>24</sup>

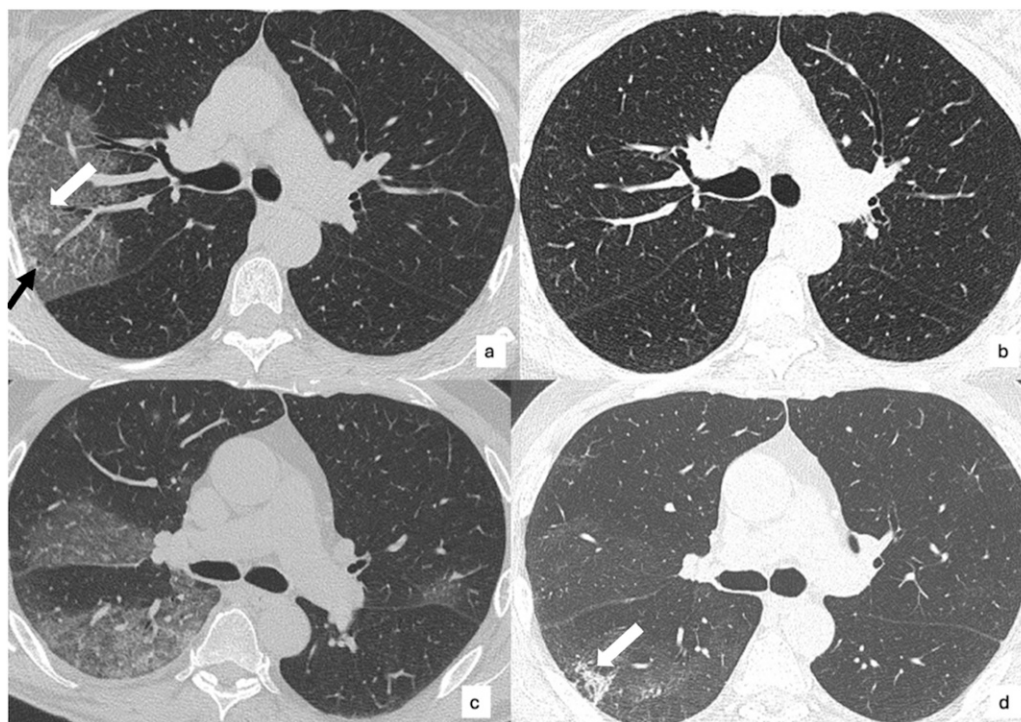


**Figure 1.** Chest CT findings of COVID-19 pneumonia. Patient 1 (a; b): extensive area of ground-glass opacity in the right upper lobe with a small inner area of consolidation (black arrow) and crazy paving (white arrow) at hospital admission, global CT score of 4 (a); complete resolution after 3 months (b). Patient 2 (c; d): bilateral areas of ground-glass opacities at hospital admission, global CT score of 12 (c); residual abnormalities, mainly sustained by ground-glass opacity, global CT score of 11, and a consolidation with architectural distortions and a bronchial dilation (white arrow), configuring a fibrotic-like appearance (d).

**Table 3.** CT score and differences between hospital admission and after discharge.

CT analysis	Baseline	3 months	p-value
CT global score, median (IQR)	9 (5.5)	5.2 (8.5)	.00007
Prevalent pattern			
• GGo	18/39 (46.2%)	33/39 (84.7%)	
• Consolidation	13/39 (33.3%)	2/39 (5.1%)	
• Crazy paving	7/39 (17.9%)	2/39 (5.1%)	
• Reticulation	1/39 (2.6%)	2/39 (5.1%)	
CT fib-like score, median (IQR)	3.5 (8.5)	3 (5.5)	.11
Prevalent pattern			
• GGo	10/39 (25.6%)	19/39 (48.7%)	
• Consolidation	11/39 (28.2%)	4/39 (10.3%)	
• Crazy paving	7/39 (17.9%)	2/39 (5.1%)	
• Reticulation	2/39 (5.1%)	—	
Fib-like abnormalities			
• Bronchial dilation	—	2/39 (5.1%)	
• Distortion	27/39 (69.2%)	22/39 (56.4%)	
• Honeycombing	—	—	
• Volume loss	2/39 (5.1%)	—	

CT: computed tomography; fib-like: fibrotic-like; GGo: ground-glass opacities; IQR: interquartile range.



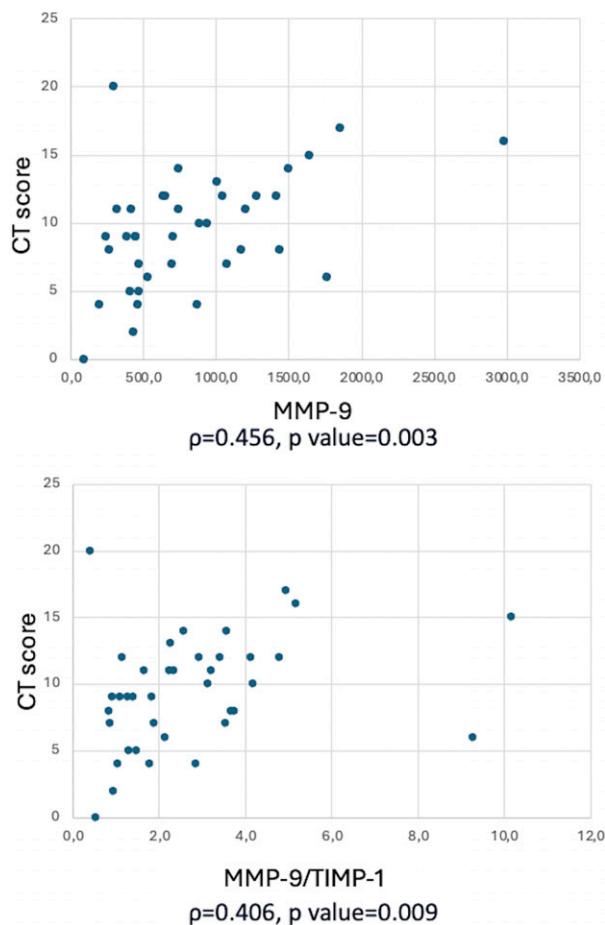


**Figure 2.** Scatter plots of correlations between MMP-9 and MMP-9/TIMP-1 ratio with CT global score at hospital admission. MMP-9: matrix metalloproteinase-9; TIMP-1: tissue inhibitor of metalloproteinase-1.

**Table 4.** Correlations between plasma enzymes at baseline and CT analysis. Significant values are in bold.

Correlations	Baseline	p-value	3 months	p-value
CT global score				
• MMP-9	<b>0.456</b>	<b>.003</b>	0.065	.689
• TIMP-1	0.275	.850	0.034	.835
• MMP-9/TIMP-1	<b>0.406</b>	<b>.009</b>	0.087	.594
CT fib-like score				
• MMP-9	0.169	.296	0.111	.496
• TIMP-1	0.034	.835	0.062	.702
• MMP-9/TIMP-1	0.087	.594	0.093	.567

In our study, fibrotic-like alterations were mainly sustained by architectural distortions, but bronchial dilation was also observed. The complete course and the underlying mechanisms of fibrotic-like alterations remain to be fully understood. Since MMPs may have a

**Table 5.** Correlations between plasma enzymes at 3 months and CT analysis.

Correlations	Baseline	p-value	3 months	p-value
CT global score				
• MMP-9	−0.048	.774	−0.095	.572
• TIMP-1	−0.103	.537	−0.016	.924
• MMP-9/TIMP-1	0.018	.916	−0.100	.552
CT fib-like score				
• MMP-9	0.003	.988	−0.163	.329
• TIMP-1	0.005	.976	−0.049	.769
• MMP-9/TIMP-1	−0.007	.969	−0.149	.372

role in the abnormal fibrotic repair processes, we sought to investigate whether MMP-9 and TIMP-1 could play a role. Our results did not confirm this hypothesis, but other MMPs could be further investigated. Moreover, it will be interesting to monitor patients with fibrotic-like alterations over time to verify if long-term residual abnormalities may indeed be considered fibrosis (e.g., progression of fibrotic signs) and to check if there is a relationship with MMP expression in these patients. In fact, since the levels of MMP-9, TIMP-1, and MMP-9/TIMP-1 did not change significantly after 3 months, an active inflammation related to COVID-19 could be still present. Hence, a longer follow-up would be desirable, excluding patients with other concomitant causes of inflammation that might influence enzymes levels during that period.

The main limitation of our study is the sample size; in fact, the sample size, computed with a power set at 80% and  $\alpha = 0.05$ , based on survival rate of COVID-19 infections admitted to the hospital in 2020 in our area,<sup>45</sup> should be at least 137. Then, longer period of follow-up would be desirable. The retrospective study design limited the availability of CT scans and blood tests at 6 or 12 months. In fact, in many cases, there was no clinical indication to repeat CT or blood tests after 6 or 12 months after hospital admission. Moreover, due to the relatively small size of our study population, we did not verify the possible influence of specific comorbidities, that could influence the results. Lastly, due to logistical limitations, we investigated only some of all possible plasma enzymes that could have a role in mid-term and long-term post COVID-19 lung alterations.

In conclusion, although we confirmed that plasma levels of MMP-9 and the MMP-9/TIMP-1 ratio during the acute phase may be related to the severity of lung involvement on CT, the absence of a significant correlation between MMP-9, TIMP-1, and the MMP-9/TIMP-1 ratio in the acute phase and residual pulmonary alterations on CT after discharge suggests that we cannot recommend their adoption as prognostic biomarkers for predicting the evolution of pulmonary involvement in COVID-19 pneumonia.

## Declaration of conflicting interests

The author(s) declared no potential conflicts of interest with respect to the research, authorship, and/or publication of this article.

## Funding

The author(s) disclosed receipt of the following financial support for the research, authorship, and/or publication of this article: Sapienza Università di Roma.

## ORCID iD

Nicholas Landini  <https://orcid.org/0000-0002-2928-3003>

## References

1. Gulick RM, Pau AK, Daar E, et al. National institutes of health COVID-19 treatment guidelines panel: perspectives and lessons learned. *Ann Intern Med* 2024; 177: 1547–1557.
2. Emanuel EJ, Persad G, Upshur R, et al. Fair allocation of scarce medical resources in the time of covid-19. *N Engl J Med* 2020; 382: 2049–2055.
3. Menter T, Haslbauer JD, Nienhold R, et al. Postmortem examination of COVID-19 patients reveals diffuse alveolar damage with severe capillary congestion and variegated findings in lungs and other organs suggesting vascular dysfunction. *Histopathology* 2020; 77: 198–209.
4. Varga Z, Flammer AJ, Steiger P, et al. Endothelial cell infection and endotheliitis in COVID-19. *Lancet* 2020; 395: 1417–1418.
5. Wichmann D, Sperhake J-P, Lütgehetmann M, et al. Autopsy findings and venous thromboembolism in patients with COVID-19: a prospective cohort study. *Ann Intern Med* 2020; 173: 268–277.
6. Middleton EA, He X-Y, Denorme F, et al. Neutrophil extracellular traps contribute to immunothrombosis in COVID-19 acute respiratory distress syndrome. *Blood* 2020; 136: 1169–1179.
7. Santos-Martínez MJ, Medina C, Jurasz P, et al. Role of metalloproteinases in platelet function. *Thromb Res* 2008; 121: 535–542.
8. Goetzl EJ, Banda MJ and Leppert D. Matrix metalloproteinases in immunity. *J Immunol* 1996; 156: 1–4.
9. Parks WC, Wilson CL and López-Boado YS. Matrix metalloproteinases as modulators of inflammation and innate immunity. *Nat Rev Immunol* 2004; 4: 617–629.
10. Parsons SL, Watson SA, Brown PD, et al. Matrix metalloproteinases. *Br J Surg* 1997; 84: 160–166.
11. Overall CM. Regulation of tissue inhibitor of matrix metalloproteinase expression. *Ann N Y Acad Sci* 1994; 732: 51–64.
12. Pi P, Zeng Z, Zeng L, et al. Molecular mechanisms of COVID-19-induced pulmonary fibrosis and epithelial-mesenchymal transition. *Front Pharmacol* 2023; 14: 1218059.
13. Beltrán-García J, Osca-Verdegal R, Pallardó FV, et al. Sepsis and coronavirus disease 2019: common features and anti-inflammatory therapeutic approaches. *Crit Care Med* 2020; 48: 1841–1844.
14. Duda I, Krzych Ł, Jędrzejowska-Szypułka H, et al. Plasma matrix metalloproteinase-9 and tissue inhibitor of matrix metalloproteinase-1 as prognostic biomarkers in critically ill patients. *Open Med* 2020; 15: 50–56.
15. Aguirre A, Blázquez-Prieto J, Amado-Rodríguez L, et al. Matrix metalloproteinase-14 triggers an anti-inflammatory proteolytic cascade in endotoxemia. *J Mol Med (Berl)* 2017; 95: 487–497.
16. Ding L, Guo H, Zhang C, et al. Elevated matrix metalloproteinase-9 expression is associated with COVID-19 severity: a meta-analysis. *Exp Ther Med* 2023; 26: 545.
17. Cavalcante GL, Bonifacio LP, Sanches-Lopes JM, et al. Matrix metalloproteinases are associated with severity of disease among COVID-19 patients: a possible pharmacological target. *Basic Clin Pharmacol Toxicol* 2024; 134: 727–736.
18. Avila-Mesquita DC, Couto AES, Campos LCB, et al. MMP-2 and MMP-9 levels in plasma are altered and associated with mortality in COVID-19 patients. *Biomed Pharmacother* 2021; 142: 112067.
19. Carvalho A, Cunha R, Lima BA, et al. Chest CT imaging features of COVID-19 pneumonia: first radiological insights from Porto, Portugal. *Eur J Radiol Open* 2020; 7: 100294.
20. Masci GM, Izzo A, Bonito G, et al. Chest CT features of COVID-19 in vaccinated versus unvaccinated patients: use of CT severity score and outcome analysis. *Radiol Med* 2023; 128: 934–943.
21. Masci GM, Iafrate F, Ciccarelli F, et al. Tocilizumab effects in COVID-19 pneumonia: role of CT texture analysis in quantitative assessment of response to therapy. *Radiol Med* 2021; 126: 1170–1180.
22. Leonardi A, Scipione R, Alfieri G, et al. Role of computed tomography in predicting critical disease in patients with covid-19 pneumonia: a retrospective study using a semiautomatic quantitative method. *Eur J Radiol* 2020; 130: 109202.
23. Murphy MC and Little BP. Chronic pulmonary manifestations of COVID-19 infection: imaging evaluation. *Radiology* 2023; 307: e222379.
24. Martini K, Larici AR, Revel MP, et al. COVID-19 pneumonia imaging follow-up: when and how? A proposition from ESTI and ESR. *Eur Radiol* 2022; 32: 2639–2649.
25. Zingaropoli MA, Latronico T, Pasculli P, et al. Tissue inhibitor of matrix metalloproteinases-1 (TIMP-1) and pulmonary involvement in COVID-19 pneumonia. *Biomolecules* 2023; 13: 1040.
26. Davey A, McAuley DF and O’Kane CM. Matrix metalloproteinases in acute lung injury: mediators of injury and drivers of repair. *Eur Respir J* 2011; 38: 959–970.
27. Fligel SEG, Standiford T, Fligel HM, et al. Matrix metalloproteinases and matrix metalloproteinase inhibitors in acute lung injury. *Hum Pathol* 2006; 37: 422–430.

28. Pan F, Ye T, Sun P, et al. Time course of lung changes at chest CT during recovery from coronavirus disease 2019 (COVID-19). *Radiology* 2020; 295: 715–721.
29. Francone M, Iafrate F, Masci GM, et al. Chest CT score in COVID-19 patients: correlation with disease severity and short-term prognosis. *Eur Radiol* 2020; 30: 6808–6817.
30. Shi H, Han X, Jiang N, et al. Radiological findings from 81 patients with COVID-19 pneumonia in Wuhan, China: a descriptive study. *Lancet Infect Dis* 2020; 20: 425–434.
31. Polak SB, Van Gool IC, Cohen D, et al. A systematic review of pathological findings in COVID-19: a pathophysiological timeline and possible mechanisms of disease progression. *Mod Pathol* 2020; 33: 2128–2138.
32. Antonio GE, Wong KT, Chu WCW, et al. Imaging in severe acute respiratory syndrome (SARS). *Clin Radiol* 2003; 58: 825–832.
33. Das KM, Lee EY, Singh R, et al. Follow-up chest radiographic findings in patients with MERS-CoV after recovery. *Indian J Radiol Imag* 2017; 27: 342–349.
34. Iannetta M, Zingaropoli MA, Latronico T, et al. Dynamic changes of MMP-9 plasma levels correlate with JCV reactivation and immune activation in natalizumab-treated multiple sclerosis patients. *Sci Rep* 2019; 9: 311.
35. Petrella C, Zingaropoli MA, Ceci FM, et al. COVID-19 affects serum brain-derived neurotrophic factor and neurofilament light chain in aged men: implications for morbidity and mortality. *Cells* 2023; 12: 655.
36. Wasilewski PG, Mruk B, Mazur S, et al. COVID-19 severity scoring systems in radiological imaging - a review. *Pol J Radiol* 2020; 85: e361–e368.
37. Ai T, Yang Z, Hou H, et al. Correlation of chest CT and RT-PCR testing for coronavirus disease 2019 (COVID-19) in China: a report of 1014 cases. *Radiology* 2020; 296: E32–E40.
38. Han X, Fan Y, Alwalid O, et al. Six-month follow-up chest CT findings after severe COVID-19 pneumonia. *Radiology* 2021; 299: E177–E186.
39. Tang D, Comish P and Kang R. The hallmarks of COVID-19 disease. *PLoS Pathog* 2020; 16: e1008536.
40. Apparailly F, Noël D, Millet V, et al. Paradoxical effects of tissue inhibitor of metalloproteinases 1 gene transfer in collagen-induced arthritis. *Arthritis Rheum* 2001; 44: 1444–1454.
41. Mostafa Mtairag E, Chollet-Martin S, Oudghiri M, et al. Effects of interleukin-10 on monocyte/endothelial cell adhesion and MMP-9/TIMP-1 secretion. *Cardiovasc Res* 2001; 49: 882–890.
42. Demir NA, Kirik SY, Sumer S, et al. An evaluation of matrix metalloproteinase-9 (Mmp-9) and tissue inhibitor metalloproteinase-1 (Timp-1) serum levels and the Mmp-9/Timp-1 ratio in Covid-19 patients. *Afr Health Sci* 2023; 23: 37–43.
43. Chiang T-Y, Yu Y-L, Lin C-W, et al. The circulating level of MMP-9 and its ratio to TIMP-1 as a predictor of severity in patients with community-acquired pneumonia. *Clin Chim Acta* 2013; 424: 261–266.
44. Landini N, Orlandi M, Fusaro M, et al. The role of imaging in COVID-19 pneumonia diagnosis and management: main positions of the experts, key imaging features and open answers. *J Cardiovasc Echogr* 2020; 30: S25–S30.
45. Istituto Superiore di Sanità. EpiCentro - L'epidemiologia per la sanità pubblica. Coronavirus. Available at: <https://www.epicentro.iss.it/coronavirus/2020> (accessed 25 March 2025).